tvst

Glaucoma

Moving Stimulus Perimetry: A New Functional Test for Glaucoma

Stuart K. Gardiner[1] **and Steven L. Mansberger**[1]

[1] Devers Eye Institute, Legacy Health, Portland, OR, USA

Correspondence: Stuart Gardiner, Devers Eye Institute, Legacy Research Institute, 1225 NE 2nd Ave, Portland, OR 97232, USA. e-mail: sgardiner@deverseye.org

Received: June 14, 2022
Accepted: August 30, 2022
Published: October 6, 2022

Keywords: automated perimetry; diagnostic testing; glaucoma

Citation: Gardiner SK, Mansberger SL. Moving stimulus perimetry: A new functional test for glaucoma. Transl Vis Sci Technol. 2022;11(10):9, https://doi.org/10.1167/tvst.11.10.9

Purpose: Static pointwise perimetric sensitivities of less than approximately 19 dB are unreliable in glaucoma owing to excessive variability. We propose using moving stimuli to increase detectability, decrease variability, and hence increase this dynamic range.

Methods: A moving stimulus was designed to travel parallel to the average nerve fiber bundle orientation at each location, and compared against an otherwise identical static stimulus. To assess dynamic range, psychometric functions were measured at 4 locations of each of 10 subjects. To assess clinically realistic test–retest variability, 34 locations of 94 subjects with glaucoma and glaucoma suspects were tested twice, 6 months apart. Pointwise sensitivity estimates were compared using generalized estimating equation regression models. The test–retest limits of agreement for each stimulus were assessed, adjusted for within-eye clustering.

Results: Using static stimuli, 9 of the 40 psychometric functions had less than a 90% maximum response probability, suggesting being beyond the dynamic range. Eight of those locations had asymptotic maximum of more than 90% with moving stimuli. Sensitivities were higher for moving stimuli ($P < 0.001$); the difference increased as sensitivity decreased ($P < 0.001$). Test-retest limits of agreement were narrower for moving stimuli (−6.35 to +6.48 dB) than static stimuli (−12.7 to +7.81 dB). Sixty-two percent of subjects preferred using moving stimuli versus 19% who preferred static stimuli.

Conclusions: Using a moving stimulus increases perimetric sensitivities in regions of glaucomatous loss. This extends the effective dynamic range, allowing reliable testing later into the disease. Results are more repeatable, and the test is preferred by most subjects.

Translational Relevance: Moving stimuli allow reliable testing in patients with more severe glaucoma than currently possible.

Introduction

Functional testing remains an essential part of clinical care in glaucoma,[1] most commonly in the form of static automated perimetry.[2] This is particularly true in eyes with more advanced damage, owing to the limited dynamic range of structural testing such as ocular coherence tomography.[3] However, results from automated perimetry have high test–retest variability at moderately or severely damaged locations.[4,5] Accurately monitoring the rate of progression at such locations is crucial for clinical management owing to their potential impact on the patient's prognosis and quality of life.[6–8] Therefore, it is important to develop new perimetric techniques that can reliably and accurately assess functional progression in regions of moderate and severe glaucomatous loss.

We have previously shown that the effective dynamic range of standard automated perimetry, using a static stimulus, ends at 15 to 19 dB.[9] Below that, sensitivity estimates from clinical perimetry were not significantly correlated with those obtained more accurately using frequency-of-seeing curves. Part of the reason for this is that the upper asymptote of the psychometric function, that is, the maximum response probability that would be predicted for an arbitrarily high contrast stimulus, was significantly lower than 100% at many such locations (light scatter from very high contrast stimuli can cause an increase in detection

from distant healthier visual field locations, but these responses are uninformative for estimating sensitivity at the location being tested). This means that stimulus detection remains probabilistic rather than deterministic, and hence estimates of sensitivity are too variable to be considered reliable. The conclusion that the effective dynamic range ends at 15 to 19 dB has been supported by subsequent analyses showing that censoring sensitivities below that point does not adversely affect the ability to monitor disease progression.[10,11] We subsequently showed that this same limit of 15 to 19 dB also applied when increasing stimulus size, from the commonly used size III target (a 0.43° diameter circle) to the alternative size V target (a 1.72° diameter circle); however, the higher sensitivities obtained with the larger stimulus meant that this limit was not reached until later in the disease process.[12]

In this study, we introduce an alternative approach to further extend the dynamic range of perimetry: increasing sensitivity by introducing motion. Moving stimuli may be easier to detect than static stimuli of the same contrast.[13] Stato-kinetic dissociation has been described both in normal[14] and glaucomatous eyes.[15,16] Sensitivities are reported to be higher for moving stimuli than static stimuli, so long as stimulus velocity is not too fast.[17–19] We anticipate an even greater effect in regions damaged by glaucoma, where the primary limiting factor for sensitivity is the remaining number of healthy retinal ganglion cells (RGCs). If the stimulus moves, it will additionally stimulate motion-sensitive RGCs.[20] Further, the remaining RGCs stimulate not only cortical mechanisms responsible for detecting stimulus onset and offset,[21] but also the middle temporal neurons responsible for motion detection,[22,23] potentially further increasing the probability of detection and reducing variability.

The moving stimulus that we describe appears at a predefined location, moves at constant speed toward a second location, then turns off. We hypothesize that this technique will increase detectability and hence increase sensitivity for a given level of RGC loss, further delaying the time at which a location had progressed beyond the effective dynamic range of the test. So long as the moving stimulus only stimulates RGCs within the same nerve fiber bundle, which evidence from adaptive optics imaging suggests are lost concurrently,[24,25] this should not impair the ability to monitor progression or to detect defects. The task for subjects is the same seen/not seen paradigm as in current clinical perimetry, aiming to measure the contrast necessary for the stimulus to be detected on 50% of presentations (unlike kinetic perimetry, where the task is to respond as soon as a stimulus is seen, and the location at which it was seen is recorded). Here, we test two resultant hypotheses about use of this moving stimulus for perimetry. In experiment 1, we test the hypothesis that the use of a moving stimulus will extend the effective dynamic range of perimetry, compared with using an otherwise identical static stimulus. In experiment 2, we test the hypothesis that use of a moving stimulus will decrease test–retest variability when still within the effective dynamic range.

Methods

Characteristics of the Moving Stimulus

The moving stimulus used at each location was defined as:

- The stimulus travels in a straight line parallel to the average nerve fiber bundle orientation at each location. Clinical perimetry most commonly uses a size III stimulus (0.43° diameter), presented at a set of predefined locations. For the 24-2 grid used by the Humphrey Field Analyzer perimeter (HFA; Carl-Zeiss Meditec Inc, Dublin, CA, USA) the interlocation spacing is 6° spacing both horizontally and vertically. At each of those same 52 locations (i.e., excluding the two locations at 15° temporal and ±3° vertical which coincide with the approximate position of the blind spot), the average orientation of nerve fiber bundles was calculated using the equations of Jansonius et al.[26] For locations temporal of the blind spot, at which the Jansonius model is not defined, it was assumed that bundles travel in a straight line emanating from the center of the optic nerve head. These orientations were then transformed from retinal orientation to visual field orientation to obtain the desired direction of stimulus motion.
- The stimulus lasts 500 ms. This is longer than the standard stimulus duration used in clinical perimetry (200 ms), because firmware limitations on the Octopus perimeter (Haag-Streit Inc, Köniz, Switzerland) used for the experiments mean that responses occurring after the end of the moving stimulus are not recorded. The longer duration used in these experiments should reduce false negatives (the proportion of "seen" responses that are missed), because it gives the subject more time to respond and still have their response recorded. A consequence of using a 500-ms stimulus is that the technician administering the test had to be alert to fixation movements visible on the instrument's camera. If fixation was noticeably unstable during the test, the technician performing the test would

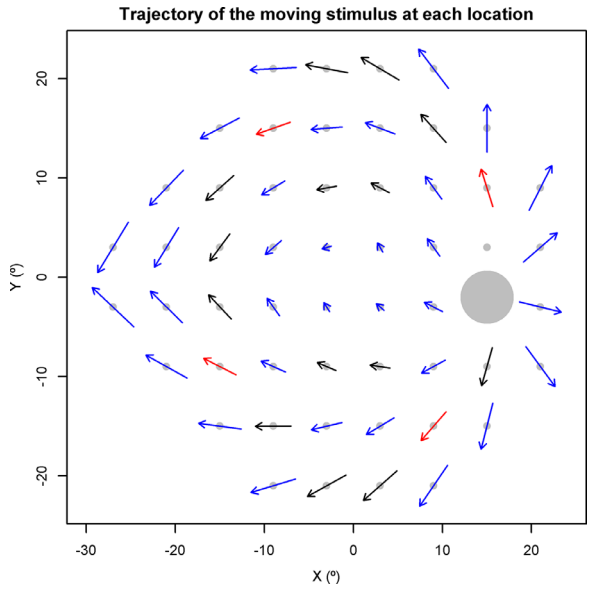

Figure 1. The trajectory of the moving stimulus at each location in the 24-2 visual field. The stimulus moves from the tail toward the head (point) of the arrow, at a constant speed, over 500 ms. Stimulus speed, and hence distance travelled, increases with eccentricity. The large gray spot indicates the approximate location of the blind spot. Locations with red arrows were those tested (using size III stimuli) in experiment 1; locations with blue arrows were those tested (using size V stimuli) in experiment 2.

first remind the subject about the importance of fixation (which is often sufficient if the instability was due to fatigue and fading attention), and, if it persisted. the test would be redone or abandoned.

- At locations (±9°, ±15°), the stimulus travels at 5°/s, moving away from the blind spot. That is, starting 1.25° closer to the blind spot than the designated location, passing through the designated location (±9°, ±15°) after 250 ms, and ending 1.25° further from the blind spot than the designated location after 500 ms.
- At other locations, the speed at which the stimulus moves was scaled in proportion to 1/M, where M represents the cortical magnification factor, to make stimuli of the same contrast approximately equally resolvable across the visual field.[27] Different formulae for M have been proposed. We used that of Horton and Hoyt,[28] who estimated that M = 17.3/(Eccentricity + 0.75). Thus, to obtain a speed of 5°/s at the aforementioned locations with Eccentricity 17.5°, the stimulus speed was set to equal (Eccentricity + 0.75)/(17.5 + 0.75) * 5°/s.

The resultant stimulus path traversed within 0.5s at each location in the 24-2 visual field is shown in Figure 1. See Supplementary Movie S1 for an example of the moving stimulus, and Supplementary Movie S2 for an example of the static stimulus presented at the same location.

Experiment 1: Effective Dynamic Range

Frequency-of-seeing curves were measured at each of the four locations shown by red arrows in Figure 1 (one in each quadrant of the visual field, at equal eccentricity, to maintain a reasonable level of spatial uncertainty[29] and encourage stable central fixation), for both moving and static stimuli. The moving stimulus was a size III target, presented for 500 ms, moving at constant speed 5°/s along the trajectory shown in Figure 1, as described elsewhere in this article. The static stimulus was also presented for 500 ms, and was identical in all respects except movement, and was presented at the midpoint of the moving stimulus' trajectory.

First, for each stimulus type in turn, a 10-presentation Zippy estimation by sequential testing (ZEST) algorithm was used to obtain an estimate of sensitivity, $Sens_{Est}$, at each of the four locations. The ZEST algorithm assumed that the sensitivity lies in the range of 10 to 40 dB; had a flat initial prior distribution over that range; and assumed that the variability for a location with a given sensitivity $Sens_{True}$ equals that predicted by Henson et al.,[30] namely, that the true psychometric function is represented by a cumulative Gaussian with mean $Sens_{True}$ and standard deviation $exp(-0.081*Sens_{True} + 3.27)$, except that this variability remains constant for a $Sens_{True}$ of less than 15 dB.[31] Next, 10 stimulus presentations were made at each of four contrasts per location: ($Sens_{Est}$ − 10), ($Sens_{Est}$ − 4), $Sens_{Est}$, and ($Sens_{Est}$ + 4) dB, with stimulus order randomized across locations and contrasts. These were interspersed with five 40-dB stimuli used to measure the false-positive response rate; thus, there were 165 stimulus presentations per run. Three such runs were performed using static stimuli, and three runs using moving stimuli, with the order of the runs randomized, and the subject allowed breaks between runs to decrease fatigue.

At each of the four locations, the response probability at each of the four selected contrasts was calculated based on the 30 stimulus presentations per contrast (i.e., combining all three runs). These were fit to a cumulative Gaussian psychometric function,[9] with lower asymptote set to equal the measured false-positive rate, and upper asymptote as a free parameter constrained to be 100% or less. From these fits, we extracted the sensitivity (contrast giving 50% response probability) and interquartile range (change in contrast needed to increase the response probability from 25% to 75%). Note that, if the upper asymptote is less than 50%, sensitivity cannot be defined.

Ten subjects were tested, taken from the Portland Progression Project cohort.[32,33] Subjects had a clinical diagnosis of primary open angle glaucoma, no other causes of visual field defect (other than mild cataract), and had a history of providing reliable test results. For inclusion in experiment 1, subjects had to have a sensitivity greater than 0 dB and 15 dB or greater at one or more of the four locations to be tested (the red locations in Fig. 1), on their most recent HFA 24-2 Swedish Interactive Thresholding Algorithm Standard visual field test. This last criterion was designed to identify subjects who may be beyond the lower limit of the effective dynamic range of perimetry. Testing was conducted on an Octopus perimeter controlled by a custom-written program in R[34] via the Open Perimetry Interface,[35] with fixation monitored continuously by the technician using the device's inbuilt camera. All testing for both experiments was approved by the local institutional review board, and adhered to the tenets of the Declaration of Helsinki.

Experiment 2: Test–Retest Variability

This experiment seeks to assess the difference in test–retest variability between moving and static stimuli when still within the effective dynamic range. For this, a clinically realistic ZEST algorithm was used. At four "seed points" located at (±9°, ±9°), the same ZEST algorithm as in the first part of experiment 1 was used, but with five stimulus presentations per location. Next, for each of the remaining locations, an initial prior probability density function was generated proportional to $0.1 + \varphi(x)$. Here, $\varphi(x)$ represents the probability density function of a Gaussian distribution with mean equal to the average of the sensitivity estimates already obtained at neighboring locations, and standard deviation equal to double the standard deviation that would be predicted for a psychometric function if that average exactly equaled the true sensitivity using the same formula as above.[30] A similar ZEST algorithm with four stimulus presentations was then conducted at that location, but using this initial prior distribution. Thus, information from neighboring locations is being used to make the testing algorithm more efficient. To keep the test time to approximately 5 minutes per eye (similar to clinical perimetry), only 34 locations were tested, as indicated by the blue arrows on Figure 1.

Subjects in the Portland Progression Project with clinical diagnoses of glaucoma or glaucoma suspect were tested at consecutive visits, 6 months apart; thus, the test–retest variability measured comprises both short-term and long-term variability.[36,37] The worst eye, according to the mean deviation from their most recent previous HFA visual field test, was used for testing. On each visit, they underwent testing with the algorithm outlined elsewhere in this article, once using moving stimuli, and once using otherwise identical static stimuli, in random order. To maximize the proportion of locations that were within the effective dynamic range, a 500 ms size V stimulus was used for both moving and static stimuli for this experiment. On each visit, after completing both tests, subjects were asked verbally which of the two they preferred.

The difference between sensitivity estimates from moving versus static stimuli was assessed using a generalized estimating equation (GEE) linear model,[38] accounting for multiple locations and two test dates per eye. Test–retest variability was defined as the difference between the first and second test dates, at each location. Bland–Altman plots of agreement[39] were created for both stimulus types, with the 95% limits of agreement adjusted for clustering of multiple locations within the same eye.[40] All analysis were performed in R version 4.0.3.[34]

Results

Experiment 1: Effective Dynamic Range

Figure 2 shows the psychometric functions measured at four locations for 1 of the 10 subjects in experiment 1. At all four locations, the moving stimulus (results shown in red) gave consistently higher

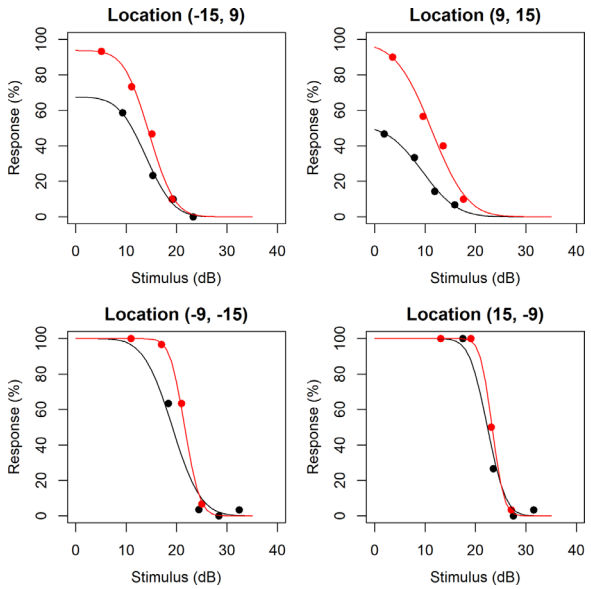

Figure 2. Psychometric functions measured at four locations of the same subject using a moving stimulus (*red*) and an otherwise-identical static stimulus (*black*).

response probabilities for the same stimulus contrast than the static stimulus (results shown in black). Consequently, the red fitted curves are shifted to the right, giving a higher sensitivity (the stimulus contrast giving 50% response probability). Notably, the psychometric functions for moving stimuli were also steeper, which would be expected to reduce test–retest variability in a clinical testing algorithm. At locations (−15°, 9°) and (9°, 15°), the asymptotic maximum response probability that would be expected for an arbitrarily high contrast stimulus (in the absence of extraneous responses caused by light scatter to distant locations in the visual field) was well below 100% for the static stimulus, indicating that the location had progressed beyond the effective dynamic range; while this asymptotic maximum was still near 100% for the moving stimulus.

Figure 3 compares the sensitivity estimates, and asymptotic maximum response probabilities, obtained at the 4 locations of all 10 subjects. Sensitivities were higher using the moving stimulus at 36 of the 37 instances when it was defined (i.e., when the maximum was >50% for both stimuli); the mean difference was 3.4 dB, with a P of less than 0.001 from GEE linear regression. The interquartile range was narrower with the moving stimulus at 30 of the 34 instances when it was defined (i.e., when the maximum was >75% for both stimuli); the mean difference was 3.2 dB ($P = 0.002$). At most locations, the fitted asymptotic maximum was 99% or more for both stimulus types, suggesting that accurate sensitivities could be obtained from the psychometric function and hence also from a clinical thresholding algorithm. However, this maximum was less than 90% for nine locations using the static stimulus, which would introduce considerable variability into any thresholding algorithm, suggesting that the location is beyond the effective dynamic range for that stimulus type. Indeed, for three locations the maximum was less than 50%, such that the detection threshold is undefined and so no estimate can be considered reliable. By contrast, only one location had a maximum of less than 90% using the moving stimulus. Thus, there were eight locations that were beyond the effective dynamic range for the static stimulus that remained within the effective dynamic range using the moving stimulus.

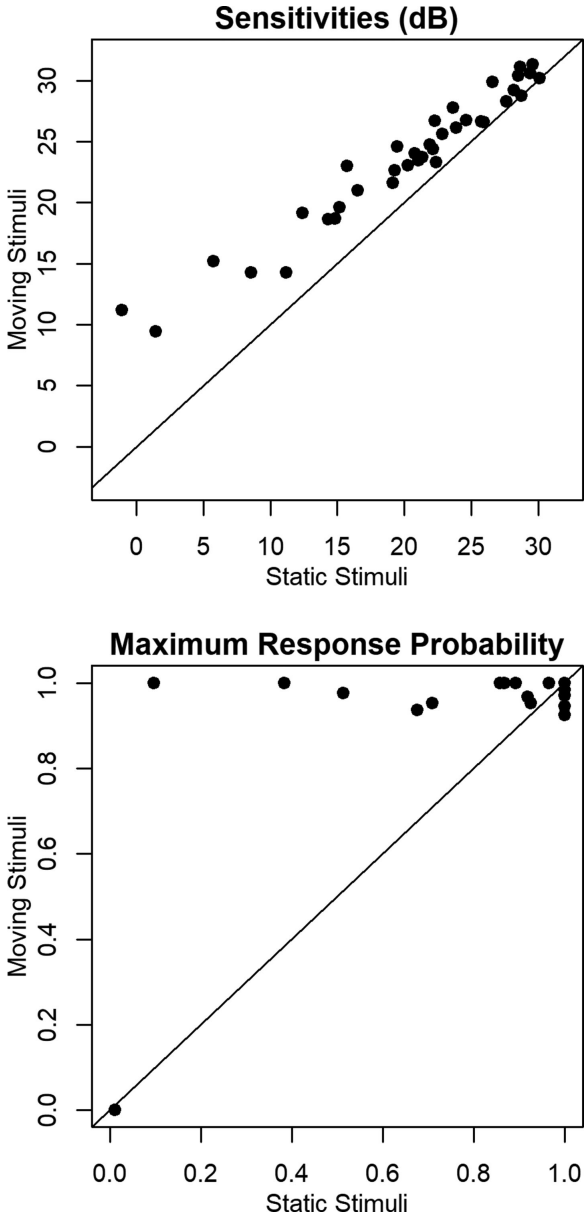

Figure 3. Comparison of psychometric functions measured at the same locations using moving versus static stimuli. (*Top*) Sensitivities, defined as the contrast (in dB) giving 50% response probability. (*Bottom*) The asymptotic maximum response probability for an arbitrarily high contrast stimulus, in the absence of extraneous responses caused by light scatter to distant visual field locations. The solid line shows the line of equality in both plots.

Experiment 2: Test–Retest Variability

We tested 94 subjects twice with the clinically realistic ZEST algorithm, 6 months apart. The average age on their second visit was 72.9 (range, 52.0–91.0 years). The average mean deviation from their HFA visual field (averaged across the two test dates) was −3.16 dB, with standard deviation 4.59 dB. Of the tested locations, 32.8% were abnormal with a P value of 5% or less on the total deviation plot on at least one of the two test dates, and 18.2% were abnormal with a P value of 1% or less.

Sensitivities using the moving stimulus were on average 1.33 dB higher, but this difference depended

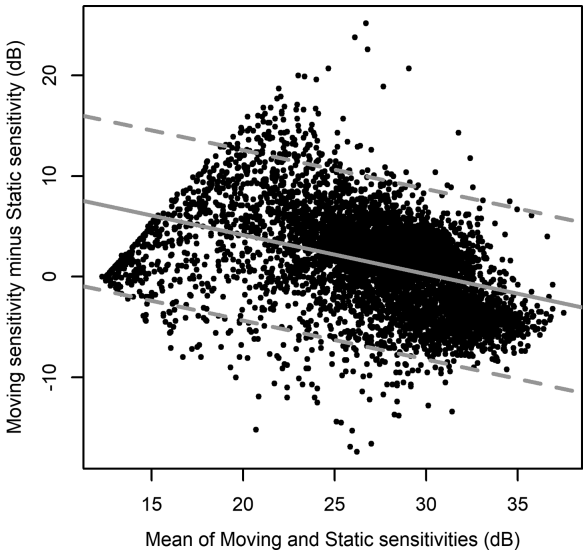

Figure 4. Bland–Altman plot comparing pointwise sensitivities obtained using moving versus static stimuli in a clinically realistic testing algorithm. Note that the lower limit of possible sensitivities in the chosen algorithm was 12.3 dB. Hence if the mean of the two sensitivities is, for example, 14.3 dB, the difference between the two cannot possibly be larger than 4 dB; this causes the apparent range of differences to appear artefactually smaller at lower sensitivities. The *solid gray line* indicates the best fit from a GEE linear model; *dashed lines* show the 95% prediction interval.

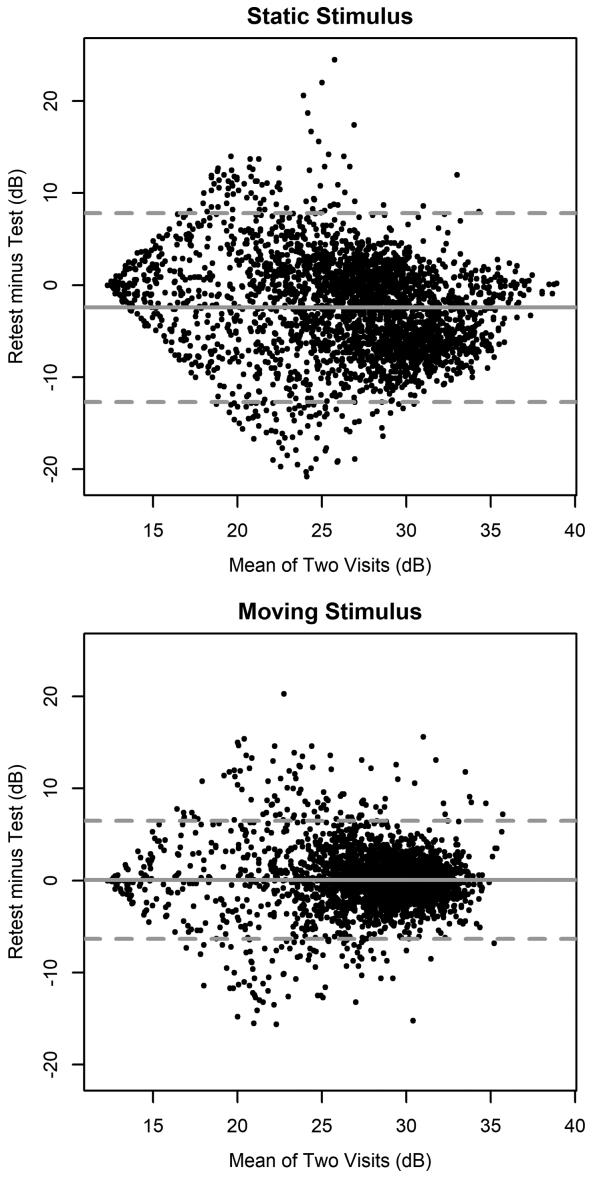

Figure 5. Bland–Altman plots showing test–retest variability for static (*top*) and moving (*bottom*) stimuli in a clinically realistic testing algorithm. *Solid gray lines* indicate the mean difference; *dashed lines* show the 95% limits of agreement adjusted for the presence of data from 34 locations per eye.

on severity. Figure 4 shows a Bland–Altman plot[39] comparing sensitivities obtained using the two stimulus types. The difference in sensitivities was higher at more damaged locations ($P < 0.001$, GEE linear regression). The difference was also greater at higher eccentricities ($P < 0.001$); this is because the speed of the moving stimulus is scaled with eccentricity (see Fig. 1) to give approximately equal normal sensitivities at each location, whereas for the static stimulus normal sensitivities are lower peripherally. In a bivariable model, both sensitivity and eccentricity were significantly related to the difference between the stimulus types ($P < 0.001$ and $P = 0.007$, respectively).

Figure 5 shows the test–retest variability, in the form of Bland–Altman plots,[39] for each stimulus type. The 95% limits of agreement, adjusted for intereye clustering of data,[40] were −12.7 to +7.81 dB for static stimuli and −6.35 to +6.48 dB for moving stimuli. The mean absolute test–retest difference was 4.48 dB for static stimuli and 2.20 dB for moving stimuli (difference $P < 0.001$, GEE regression). The proportion of locations of less than 19 dB (either owing to variability, or owing to being beyond the dynamic range) was 12.8% for static stimuli versus 5.8% for moving stimuli ($P < 0.001$, Obuchowski's test for clustered proportions).[41] The proportion of locations of more than 35 dB (which are almost certainly owing to variability) was 5.8% for static stimuli versus 0.5% for moving stimuli ($P < 0.001$).

Figure 6 shows histograms of which stimulus type subjects reported preferring at each of their two visits. Consistently, more subjects preferred the moving stimulus test. Notably, the proportion who preferred the moving stimulus increased on their second visits, suggesting that the preference was not just due to novelty of the task.

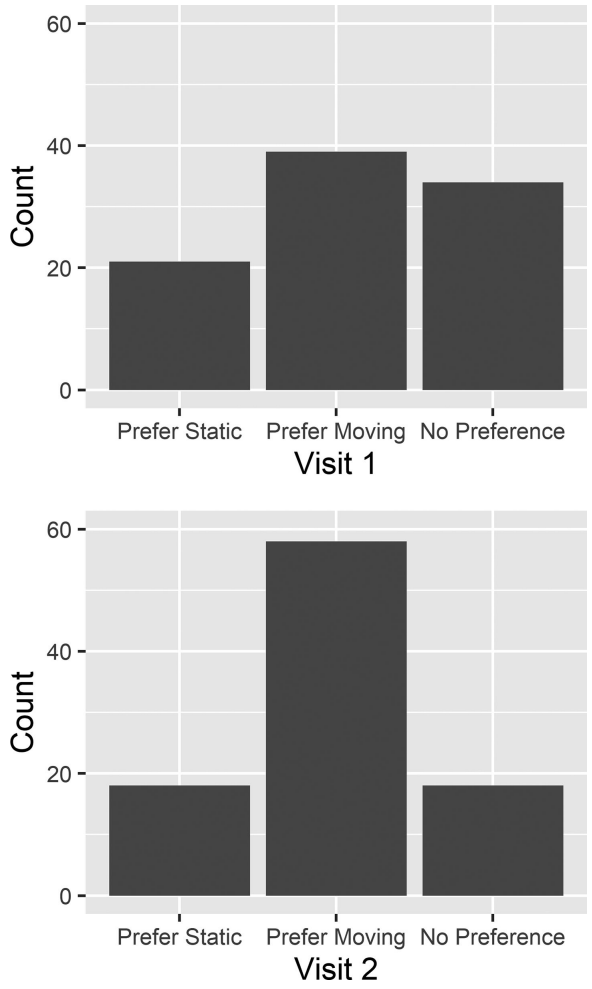

Figure 6. Histograms showing which stimulus type subjects subjectively preferred, after completing both tests, on each of the two visits.

Discussion

In these two experiments, we found that performing automated perimetry with a moving stimulus gave higher sensitivities and lower variability than a static stimulus, when all other aspects of the testing were kept the same including the instrument, testing paradigm, and test algorithm. This both extended the dynamic range into locations with more advanced disease (experiment 1), and reduced test–retest variability while within the dynamic range (experiment 2).

Most subjects in the study reported preferring testing with the moving stimulus. This preference strengthened, from 42% on the first visit to 62% on the second visit, suggesting that it is not purely due to the novelty of the test. One reason for this preference may be gleaned from the psychometric functions measured in experiment 1. The static stimulus resulted in wider interquartile ranges at most locations. This factor increases the range of stimuli, and hence the proportion of stimulus presentations, over which the subject is unsure whether they saw the stimulus or not. That subjective uncertainty can be stressful for the subject, leading them to prefer the moving stimulus test which causes them less uncertainty. The stress would also be expected to increase fatigue, and hence increase variability.[42] Perimetry has always been endured rather than enjoyed by patients[43]; even a modest improvement in the patient experience would be welcomed by many, and it may also improve the diagnostic information available to clinicians.

Testing for both experiments was conducted on an Octopus perimeter, controlled via the Open Perimetry Interface.[35] Using a clinical instrument, and the same seen/not seen testing paradigm as in clinical perimetry means that the test is more familiar to subjects, which would be expected to allow more reliable results; in addition, the conclusions are more immediately translatable to clinical care. However, testing relied on the current firmware programmed into the Octopus perimeter. Notably, this means that, for the moving stimulus, the response window during which the subject's responses (in the form of button pushes) were recorded only lasted for the time when the stimulus was present, because the firmware treats it as a kinetic perimetry stimulus. By contrast for the static stimulus, the response window extended 500 ms after the stimulus turned off. This will have caused some valid responses to be missed for the moving stimulus, especially near the detection threshold where the off detection pathway may produce a larger neural response than the on pathway.[21] A consequence is that sensitivities were likely underestimated for some locations using the moving stimulus. Indeed, on Figure 4 is it seen that the moving stimulus seemed to produce lower sensitivities than the static stimulus when greater than 31 dB, probably owing to this caveat. It is possible that the test–retest variability for the moving stimulus shown in Figure 5 is also an overestimate for the same reason, and hence that the benefits of using a moving stimulus in clinical perimetry are being underestimated.

A consequence of this requirement to use a 500-ms stimulus is that small movements in fixation during the presentation would be expected. As in most current clinical perimeters, individual stimulus presentations were not discarded based on fixation instability. Instead, fixation was closely monitored by the technician to ensure that the instability was not excessive. It should be noted that this caveat applies equally to the moving and static stimuli, and there is not reason to

expect fixation instability to differ significantly between the stimuli, especially because the order of testing was randomized.

The trajectory of the moving stimulus was a straight line, parallel to the average nerve fiber bundle orientation at that location, according to the map of Jansonius et al.[26] That map was derived by tracing nerve fiber bundles on 27 deidentified fundus photos, with no adjustments for factors such as axial length that could influence the trajectories, or factors such as age and media opacity that could have selectively influenced visibility of the bundles. Their map was also spatially limited owing to the visibility of the bundles, and several test locations fall within regions at which the trajectories were extrapolated beyond the observed range of traced bundles, and/or in the nasal region at which the model is undefined. Finally, the map adjusted for the position of the optic nerve head relative to the horizontal midline, which was not taken into account here. An optimal implementation of the moving stimulus technique could instead individualize the stimulus trajectories based on the observed nerve fiber bundle orientations in that particular eye. However, there are significant obstacles to achieving this goal. The determination of bundle orientations would have to be done quickly and automatically for realistic clinical implementation, perhaps by applying artificial intelligence approaches to derive the map. The image used to perform that task would have to cover the entire 24-2 visual field with adequate visibility. The image would also have to be acquired while the subject was seated at the perimeter, because moving to a different instrument would alter the exact position of the subject on the chin rest and hence induce torsional eye movements. If these obstacles could be overcome, it seems likely (although not certain) that it would yield further improvement in the performance of the moving stimulus relative to static stimuli; hence, again our results are conservative and the benefits of moving stimuli may be being underestimated.

A remaining question is whether the moving stimulus impacts the ability to discriminate between eyes with healthy versus damaged visual fields. In this study, all eyes had a clinical diagnosis of either glaucoma or glaucoma suspect. Testing in healthy eyes is underway to answer that question. It should be noted, however, that the usefulness of the moving stimulus technique does not depend on the results of those experiments. If defect detectability with the moving stimulus is equal to, or better than, with the static stimulus, then it would be reasonable to use a stimulus whose magnitude of movement is constant, as in the current study. If defect detectability is decreased using the moving stimulus, then the distance travelled by the stimulus could simply be scaled linearly with contrast. At near-normal sensitivities, there would be near-zero stimulus motion, ensuring that defect detectability would be identical to that achieved using static stimuli; then, the amount of motion would increase as contrast increased, providing the benefits of extended dynamic range and decreased variability at damaged locations.

The speed and distance travelled of the moving stimulus used in this study was scaled by eccentricity, as seen in Figure 1. Some form of scaling is necessary; the amount of motion needed to increase sensitivity at central locations would be imperceptible at more peripheral locations. However, the optimal scaling to use is unclear. The stimulus used here was scaled based on the cortical magnification factor,[27] yet different formulae for that factor have been reported.[28,44] Further, it is not clear whether it would be better to scale the stimulus to obtain equal average sensitivities across the visual field for healthy observers, or to obtain equal lower limits of the normative range across the visual field, which may not give the same formula.[45,46] The magnitude of the difference between such formulae may be too small for its effect to be detectable with small scale experiments, so it is likely that a choice would have to be made a priori before any clinical implementation of the technique. It is not clear whether the greater distance travelled peripherally makes those locations more susceptible to variability caused by fixation instability, particularly when using a 500-ms stimulus, or whether the decreased axon bundle density peripherally makes those locations sufficiently robust to fixational movements. Adjustments could also be made to optimize the efficiency of the testing, for example, using spatial filtering to allow all 52 locations in the 24-2 visual field to be tested instead of the subset of 34 locations tested here; however, these should not alter the direct head-to-head comparisons between stimulus types performed in this study. A final caveat is that subjects in this study had a clinical diagnosis of glaucoma or glaucoma suspect, and so the usefulness of the technique in patients with other causes of vision loss is not yet known.

We have previously shown that the effective dynamic range of perimetry can be extended by using a larger stimulus. The same limit of 15 to 19 dB applied for both size III and size V stimuli, but the higher sensitivities with the larger stimulus meant that this limit was not reached as soon.[12] This approach could be extended, using ever larger stimuli to probe locations with increasing damage. In early damage, several groups have reported that size modulation perimetry shows promise, because it may have a better signal-to-noise ratio than conventional perimetry (where size remains

constant but contrast is modulated), in particular for detection of defects.[47–49] This finding is particularly true if stimuli are configured to remain smaller than Ricco's area of complete spatial summation, which expands in glaucoma.[49] However, RGC receptive fields exhibit a center-surround organization.[50,51] The neural response of an RGC increases if the center of its receptive field is stimulated, but this response is decreased if the surround is also stimulated.[21,52] This finding implies that the largest response to a perimetric stimulus comes from RGCs whose receptive field is near the edge of the stimulus, rather than those near the middle of the stimulus where both center and surround of the receptive field are stimulated. Hence, near the detection threshold it is primarily these RGCs near the stimulus edge that determine detectability. If the stimulus size is increased, it is no longer the same RGCs that are located near the edge of the stimulus. The extent of this problem with size modulation remains to be seen, and it is possible that it may be only a relatively minor caveat, especially when seeking only to distinguish defects from areas of normal sensitivity. However, the lack of location consistency could severely impair the ability to monitor glaucomatous progression. Size modulation perimetry is implicitly assuming that RGC loss is homogeneous across the extent of the stimulus (a circle several degrees across), whereas moving stimulus perimetry only relies on the much weaker assumption that RGC loss is homogeneous within the same axon bundle, as supported by advanced imaging studies.[24,25] Notably, if it is found that these caveats with size modulation perimetry are relatively minor, it would be perfectly possible to combine the two approaches, whereby a stimulus both enlarges and moves, to obtain the benefits of both.

In summary, we found that using a moving stimulus instead of a static stimulus, in an otherwise identical seen/not seen perimetric task similar to those used clinically, both extended the dynamic range into locations with more advanced disease and decreased test–retest variability while within the dynamic range. The test could be implemented on current instruments, easing translatability of the findings and making any transition easier for patients. Subjects mostly reported preferring the moving stimulus test, suggesting potential benefits for both patient satisfaction and the reliability of the results. Given the known high variability of current perimetry especially in damaged areas, and the lack of other test modalities for monitoring disease progression in regions of advanced loss, we suggest that use of a moving stimulus may improve the diagnostic usefulness of functional testing for glaucoma.

Acknowledgments

Supported by NEI R01 EY020922 (to S.K.G.); NEI R01 EY031686 (to S.K.G.); Good Samaritan Foundation.

Disclosure: **S.K. Gardiner**, Legacy Health (P); **S.L. Mansberger**, None

References

1. Stagg BC, Stein JD, Medeiros FA, et al. The frequency of visual field testing in a US nationwide cohort of individuals with open angle glaucoma. *Ophthalmol Glaucoma*. 2022 May 20:S2589-4196(22)00083–7, doi:10.1016/j.ogla.2022.05.002. Online ahead of print.
2. Heijl A, Krakau CE. An automatic perimeter for glaucoma visual field screening and control. Construction and clinical cases. *Graefes Arch Clin Exp Ophthalmol*. 1975;197(1):13–23.
3. Moghimi S, Bowd C, Zangwill LM, et al. Measurement floors and dynamic ranges of OCT and OCT angiography in glaucoma. *Ophthalmology*. 2019;126(7):980–988.
4. Heijl A, Lindgren A, Lindgren G. Test-retest variability in glaucomatous visual fields. *Am J Ophthalmol*. 1989;108(2):130–135.
5. Artes PH, Iwase A, Ohno Y, Kitazawa Y, Chauhan BC. Properties of perimetric threshold estimates from Full Threshold, SITA Standard, and SITA Fast strategies. *Invest Ophthalmol Vis Sci*. 2002;43(8):2654–2659.
6. Saunders LJ, Russell RA, Kirwan JF, McNaught AI, Crabb DP. Examining visual field loss in patients in glaucoma clinics during their predicted remaining lifetime. *Invest Ophthalmol Vis Sci*. 2014;55(1):102–109.
7. Lisboa R, Chun YS, Zangwill LM, et al. Association between rates of binocular visual field loss and vision-related quality of life in patients with glaucoma. *JAMA Ophthalmol*. 2013;131(4):486–494.
8. Medeiros FA, Gracitelli CP, Boer ER, Weinreb RN, Zangwill LM, Rosen PN. Longitudinal changes in quality of life and rates of progressive visual field loss in glaucoma patients. *Ophthalmology*. 2015;122(2):293–301.
9. Gardiner SK, Swanson WH, Goren D, Mansberger SL, Demirel S. Assessment of the reliability of standard automated perimetry in regions

of glaucomatous damage. *Ophthalmology*. 2014;121(7):1359–1369.
10. Gardiner SK, Swanson WH, Demirel S. The effect of limiting the range of perimetric sensitivities on pointwise assessment of visual field progression in glaucoma. *Invest Ophthalmol Vis Sci*. 2016;57(1):288–294.
11. Turpin A, Morgan WH, McKendrick AM. Improving spatial resolution and test times of visual field testing using ARREST. *Transl Vis Sci Technol*. 2018;7(5):35.
12. Gardiner SK, Demirel S, Goren D, Mansberger SL, Swanson WH. The effect of stimulus size on the reliable stimulus range of perimetry. *Transl Vis Sci Technol*. 2015;4(2):10.
13. Rowe F. *Methods of Visual Field Assessment. Visual Fields via the Visual Pathway*. Hoboken, NJ: Blackwell Publishing Ltd; 2008:27–51.
14. Owsley C, Sekuler R, Siemsen D. Contrast sensitivity throughout adulthood. *Vision Res*. 1983;23(7):689–699.
15. Gandolfo E, Rossi F, Ermini D, Zingirian M. Early perimetric diagnosis of glaucoma by stato-kinetic dissociation. In: Mills R, Wall M, editors. *Perimetry Update 1994/1995*. Amsterdam/New York: Kugler; 1995:271–276.
16. Gandolfo E. Stato-kinetic dissociation in subjects with normal and abnormal visual fields. *Eur J Ophthalmol*. 1996;6(4):408–414.
17. Long GM, Homolka JL. Contrast sensitivity during horizontal visual pursuit: dynamic sensitivity functions. *Perception*. 1992;21(6):753–764.
18. Sunny MM, von Muhlenen A. Motion onset does not capture attention when subsequent motion is "smooth". *Psychon Bull Rev*. 2011;18(6):1050–1056.
19. Long GM, Zavod MJ. Contrast sensitivity in a dynamic environment: effects of target conditions and visual impairment. *Hum Factors*. 2002;44(1):120–132.
20. Manookin MB, Patterson SS, Linehan CM. Neural mechanisms mediating motion sensitivity in parasol ganglion cells of the primate retina. *Neuron*. 2018;97(6):1327–1340.e4.
21. Gardiner SK, Swanson WH, Demirel S, McKendrick AM, Turpin A, Johnson CA. A two-stage neural spiking model of visual contrast detection in perimetry. *Vision Res*. 2008;48(18):1859–1869.
22. Born RT, Bradley DC. Structure and function of visual area MT. *Annu Rev Neurosci*. 2005;28:157–189.
23. Bach M, Hoffmann MB. Visual motion detection in man is governed by non-retinal mechanisms. *Vision Res*. 2000;40(18):2379–2385.
24. Chen MF, Chui TY, Alhadeff P, et al. Adaptive optics imaging of healthy and abnormal regions of retinal nerve fiber bundles of patients with glaucoma. *Invest Ophthalmol Vis Sci*. 2015;56(1):674–681.
25. Hood DC, Lee D, Jarukasetphon R, et al. Progression of local glaucomatous damage near fixation as seen with adaptive optics imaging. *Transl Vis Sci Technol*. 2017;6(4):6.
26. Jansonius NM, Nevalainen J, Selig B, et al. A mathematical description of nerve fiber bundle trajectories and their variability in the human retina. *Vision Res*. 2009;49(17):2157–2163.
27. Johnston A, Wright MJ. Visual motion and cortical velocity. *Nature*. 1983;304(5925):436–438.
28. Horton JC, Hoyt WF. The representation of the visual field in human striate cortex. A revision of the classic Holmes map. *Arch Ophthalmol*. 1991;109(6):816–824.
29. Pelli DG. Uncertainty explains many aspects of visual contrast detection and discrimination. *J Opt Soc Am A*. 1985;2(9):1508–1532.
30. Henson DB, Chaudry S, Artes PH, Faragher EB, Ansons A. Response variability in the visual field: comparison of optic neuritis, glaucoma, ocular hypertension, and normal eyes. *Invest Ophthalmol Vis Sci*. 2000;41(2):417–421.
31. Rubinstein NJ, McKendrick AM, Turpin A. Incorporating spatial models in visual field test procedures. *Transl Vis Sci Technol*. 2016;5(2):7.
32. Gardiner SK, Johnson CA, Demirel S. Factors predicting the rate of functional progression in early and suspected glaucoma. *Invest Ophthalmol Vis Sci*. 2012;53(7):3598–3604.
33. Gardiner SK, Mansberger SL, Fortune B. Time lag between functional change and loss of retinal nerve fiber layer in glaucoma. *Invest Ophthalmol Vis Sci*. 2020;61(13):5.
34. R Development Core Team. *R: A Language and Environment for Statistical Computing*, 4.0.0 ed. Vienna, Austria: The R Foundation for Statistical Computing; 2020.
35. Turpin A, Artes PH, McKendrick AM. The open perimetry interface: an enabling tool for clinical visual psychophysics. *J Vis*. 2012;12(11):22.
36. Flammer J, Drance SM, Zulauf M. Differential light threshold. Short- and long-term fluctuation in patients with glaucoma, normal controls, and patients with suspected glaucoma. *Arch Ophthalmol*. 1984;102(5):704–706.
37. Hutchings N, Wild JM, Hussey MK, Flanagan JG, Trope GE. The long-term fluctuation of the visual field in stable glaucoma. *Invest Ophthalmol Vis Sci*. 2000;41(11):3429–3436.

38. Liang K, Zeger S. Longitudinal data analysis using generalized linear models. *Biometrika*. 1986;73:13–22.
39. Bland J, Altman D. Statistical methods for assessing agreement between two methods of clinical measurement. *Lancet*. 1986;1:307–310.
40. Bland J, Altman D. Agreement between methods of measurement with multiple observations per individual. *J Biopharm Stat*. 2007;17:571–582.
41. Obuchowski NA. On the comparison of correlated proportions for clustered data. *Stat Med*. 1998;17(13):1495–1507.
42. Hudson C, Wild JM, O'Neill EC. Fatigue effects during a single session of automated static threshold perimetry. *Invest Ophthalmol Vis Sci*. 1994;35(1):268–280.
43. Gardiner SK, Demirel S. Assessment of patient opinions of different clinical tests used in the management of glaucoma. *Ophthalmology*. 2008;115(12):2127–2131.
44. Qiu A, Rosenau BJ, Greenberg AS, et al. Estimating linear cortical magnification in human primary visual cortex via dynamic programming. *Neuroimage*. 2006;31(1):125–138.
45. Heijl A, Lindgren G, Olsson J. Normal variability of static perimetric threshold values across the central visual field. *Arch Ophthalmol*. 1987;105(11):1544–1549.
46. Gardiner SK. Differences in the relation between perimetric sensitivity and variability between locations across the visual field. *Invest Ophthalmol Vis Sci*. 2018;59(8):3667–3674.
47. Hirasawa K, Shoji N, Kasahara M, Matsumura K, Shimizu K. Comparison of size modulation and conventional standard automated perimetry with the 24-2 test protocol in glaucoma patients. *Sci Rep*. 2016;6(1):25563.
48. Wall M, Doyle CK, Eden T, Zamba KD, Johnson CA. Size threshold perimetry performs as well as conventional automated perimetry with stimulus sizes III, V, and VI for glaucomatous loss. *Invest Ophthalmol Vis Sci*. 2013;54(6):3975–3983.
49. Rountree L, Mulholland PJ, Anderson RS, Garway-Heath DF, Morgan JE, Redmond T. Optimising the glaucoma signal/noise ratio by mapping changes in spatial summation with area-modulated perimetric stimuli. *Sci Rep*. 2018;8:2172.
50. Croner LJ, Kaplan E. Receptive fields of P and M ganglion cells across the primate retina. *Vision Res*. 1995;35(1):7–24.
51. Lee BB. Receptive field structure in the primate retina. *Vision Res*. 1996;36(5):631–644.
52. Pan F, Swanson WH. A cortical pooling model of spatial summation for perimetric stimuli. *J Vis*. 2006;6(11):1159–1171.

Supplementary Material

Supplementary Movie S1. Example of a moving stimulus.

Supplementary Movie S2. Example of a static stimulus.